Materials Research Proceedings 28 (2023) 1303-1312 https://doi.org/10.21741/9781644902479-141

Evaluation of the surface integrity characteristics of internal threads machined on lead-free brass alloy

ZOGHIPOUR Nima[1,2,a *], TORAMAN Yaren[1,b], KARA Koray[1,c], BAS Kaan Can[1,2,d] and KAYNAK Yusuf[2,e]

[1]Torun Metal Alloy Ind. & Ltd. Inc., GOSB, İhsan Dede St. No: 116 41480 Gebze,Kocaeli, Turkey

[2]Department of Mechanical Engineering, Marmara University, 34722 Goztepe Campus-Istanbul, Turkey

[a]nima.zoghipour@gmail.com, [b]yaren.toraman@torunmetal.com, [c]koray.kara@torunmetal.com, [d]kaan.bas@torunmetal.com, [e]yusuf.kaynak@marmara.edu.tr

Keywords: Tapping, Threading, Surface Integrity, Lead-Free Brass Alloy

Abstract. Tapping is a typical machining method being utilized in manufacturing internal threads. However, it contains few difficulties to be dealt with since during the process, many cutting edges involve synchronized axial and rotational movements. This work presents the results of an experimental study on the material type considering the influences of the manufacturing process (extrusion and forging) and tap type on the surface integrity characteristics of lead-free brass alloys. Experimental data on the surface quality of the threads, subsurface characteristics including microhardness is presented and analyzed. This study demonstrates that the manufacturing methods have a robust effect on microstructural aspects of low-lead brass alloy and resulting in hardening of the surface and subsurface.

Nomenclature

Ext.	Extruded	F+Ann.	Forged+Annealed

Introduction

In line with advancing technology, the necessity for brass alloys in industry is rising daily. A variety of these alloys are employed in the production of the parts that are primarily used in the food, water, and pumping industries. These parts are manufactured by extrusion or hot forging processes and go through machining processes such as threading in order to be assembled. Addition of some elements into the chemical composition results in enhanced machinability, one of which is Pb [1]. However, due to its use in drinking water, the element's hazardous properties have resulted in the adoption of rigorous regulations and the widespread use of Pb [2]. As a result, recent years have seen a surge in hopes for the creation of lead-free brass alloys due to the rapid advancement of technology. However, the issue that modern industry must face to stay competitive is the manufacture of consumer goods, which is built on a triangle consisting of low costs, low production times, and excellent quality. A new problem that needs to be resolved in this situation is the poor machinability. Industrial methods for producing profiled parts are constantly evolving and competing for market share based on both product quality and price. The utilization of efficient processes is required to achieve these goals [3]. Using both cut and form taps, internal threads can be produced. Cut tapping is a type of machining; chip removal produces the thread. When form tapping is used, the work material is the sole thing that moves to create the thread.

According to Fromentin et al. [4], the main benefit of form tapping is that no chips are produced. The authors claim that by doing this, time-consuming cleaning of the threaded area can be avoided because chips can cause interference when the components are assembled. In another study, the plastic strain and the high strain stress produced by the form tapping were explored by Fromentin et al. [5]. The authors came to the conclusion that form tapping is a good alternative to the conventional tapping procedure. However, it might be argued that the production of forming threads only has a significant potential for materials with high ductility. This is due to the external form tapping's superior surface and stronger threads compared to conventional tapping for thread profiles [6]. The size of the split crest at the top of the thread following the form tapping operation will depend on the diameter of the hole. Both high ductile alloys, such as non-ferrous metals [7–10], and hardened steels, as demonstrated by [7, 11], can be formed using this method. On AISI 304 austenitic stainless steel, tapping operations were performed by Uzun et al. [12] utilizing taps of various sizes and cutting parameters. The depth of cut for each cutting feed and the cutting torques generated during threading were used to calculate the cutting performances of the taps. In the tapping forming process of the 7075-T6 aluminum alloy, Oliveira et al. [13] examined the effects of the tapping speed, tap coating, and the tapered region of the tap. They used a sophisticated statistical analysis to determine the impact of the key factors on the thrust force, torque, and connection of these factors with microhardness and thread profile quality. Burr development during the form tapping process was investigated by Filho et al. [14]. With uncoated and coated taps, internal threads in workpieces made of the 7075-aluminum alloy were completed, and the burr formation at the entrance and exit was examined. The impact of new vegetable oil formulations on the precision of AISI 316L parts and the integrity of their surfaces during reaming and tapping were examined by Belluco et al. [15]. They studied surface roughness and surface metallurgy as part of their investigation of surface integrity. Profilometry was used to evaluate roughness, while optical metallography and microhardness testing were used to investigate the subsurface. The surface characteristics of the threads produced by form tapping were investigated by Fromentin et al. [4]. The two main factors affecting the process are the work material's tensile strength and the lubricant's influence, and a relationship with tapping torque was suggested. In their study, Coelho et al. [16] concentrated on the usage of a minimum quantity of lubricant and emulsion during the machine and form tapping of 7075-T651 aluminum alloy while using both tapping techniques at three forming/cutting speeds. Numerous studies on the methods of tapping various materials have been conducted [17-20].

A comparison of the various types of tools on brass alloys has not been done, according to the research that is currently available in the literature. This paper presents the findings of an experimental investigation on the material type taking into account the influences of the manufacturing method (extrusion and forging) and tap type on the surface integrity properties of lead-free brass alloys. Experimental data on cutting forces, torques, thread surface quality, geometrical accuracy, and subsurface parameters including microhardness are presented and examined.

Methodology

Materials.

Extruded CuZn40Pb2 (CW617N), CuZn38As (CW511L), and CuZn21Si3P (CW724R), each with a diameter of 60 mm and a length of 30 mm, were the three different types of brass alloys employed as test materials in this study. In a Hydromec 550 eccentric press machine with a press load of 165 tons, a portion of these materials was hot forged at 730±10°C at a rate of 11 strokes per minute. The forged specimens underwent a 150 min. annealing process at 550°C. Table 1 and 2 list the chemical composition and mechanical properties of the test materials.

Table 1. Chemical composition of the studied brass alloys [21].

Composition		Cu	Zn	Pb	Sn	Fe	Ni	Al	As	Mn	P	Si
CW617N	%Min.	57.0	Rem.	1.6	-	-	-	-	-	-		-
	%Max.	59.0	Rem.	2.5	0.3	0.3	0.3	0.05	-	-	-	-
CW511L	%Min.	61.5	Rem.	-	-	-	-	-	0.02	-	-	-
	%Max.	63.5	Rem.	0.2	0.1	0.1	0.3	0.05	0.15	-	-	-
CW724R	%Min.	75.0	Rem.	-	-	-	-	-	-	-	0.02	2.7
	%Max.	77.0	Rem.	0.09	0.3	0.3	0.2	0.05	-	0.05	0.10	3.5

Table 2. Mechanical properties of the studied brass alloys [21].

Material	*E*(GPa)	ρ (g/cm^3)	Machinability
CW617N	96	8.43	%95
CW511L	100	8.25	%80
CW724R	100	8.41	%40

Experimental setup.

The internal threading operation using Gühring's C type M10x1.5 form and cut taps on a Fanuc α-D21LiB5 CNC milling center was the main focus of the machining experiments. Fig. 1 depicts the experimental configuration. Through all holes, the experiments were the primary focus and coolant fluid was used. Throughout the testing, the spindle rotational speed was maintained at constant 800 rpm. The cutting forces were measured for 15 seconds at a sampling frequency of 100 Hz using a Kisteler dynamometer type 9129AA. Using a Keyence digital optical microscope, a Mitutoyo Contracer CV-2100M4, and other tools, the integrity of the machined surfaces was assessed. According to ASTM E 384 standards, measurements were taken using an MHVD 1000 IS microhardness tester at various depths beneath the machined surfaces. The dimensional accuracy of the threads was controlled by M10 tap gauge as well as Keyence digital optical microscope according to the illustrated Metric ISO thread dimensions as illustrated in Fig. 2.

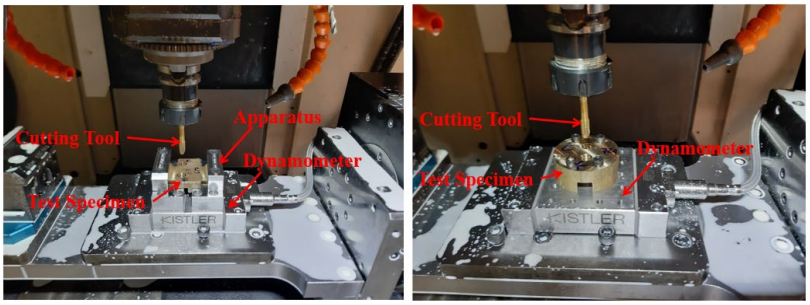

Fig. 1. The experimental setup; a) Ext., b) F+Ann. specimen.

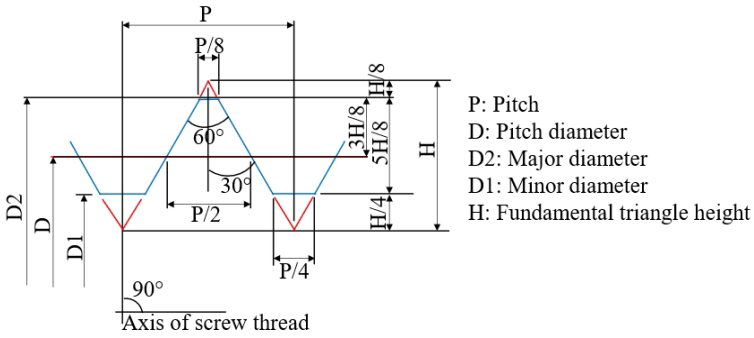

Fig. 2. Metric ISO thread control dimensions.

Results and Discussions

Microstructural Analysis.

Fig. 3 illustrates the microstructure of the Ext. and F+Ann. CW617N, CW511L, and CW724R brass alloys. α and β phases are observed in CW617N and CW511L, while α, γ and κ are seen in CW724R. The β phase content for CW617N has increased from%46 to %51 as a result of multi-directional hot forging and annealing. For CW511L, this rate was gauged between %5 and %17. This augmentation and elongation can be attributed to the phase's superplastic deformation characteristic during the forging process. In CW724R, κ and γ phases have increased from %16 to %19. The looming up of κ phase and the smaller percentages of γ phases compared to κ phases make it seem possible to ignore them and conclude that forging. Table 3 illustrates the measured average grain sizes of two test specimens. The lowest grain size was measured for F+Ann. CW724R as equal to 6.44 µm. The highest grain size was observed for Ext. CW511L as 8.13 µm. It is seen that the average grain size has been reduced by hot forging followed by annealing due to the movement of the dislocations, boundaries, breakages in grain structure and replacement with finer grains.

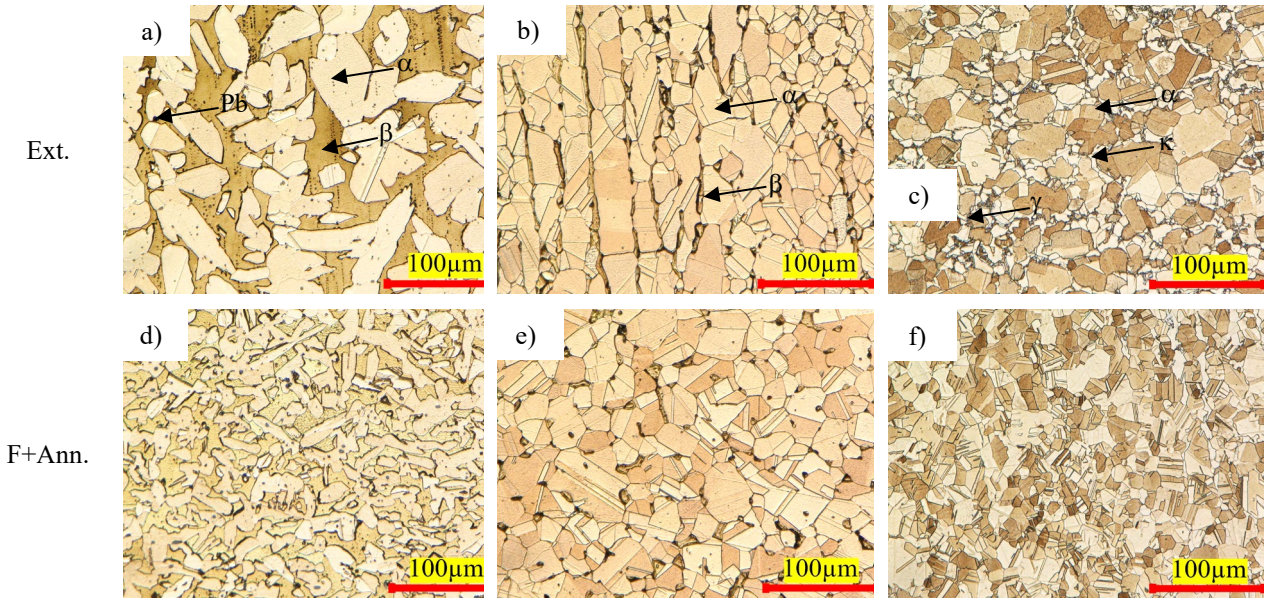

Fig. 3. Microstructure of the test speciemens; Ext.; a) CW617N, b) CW511L, c) CW724R, F+Ann.; d) F+Ann. CW617N, e) CW511L, f) CW724R.

Table 3. Measured average grain sizes and microhardness of the test specimens.

Ave. Grain size (μm)	Ext.	F+Ann.	Ave. Microhardness (HV)	Ext.	F+Ann.
CW617N	7.87	7.14		91.2	112.35
CW511L	8.31	7.74		85.5	102.80
CW724R	6.91	6.44		119	139..35

Cutting Forces and Torques Analysis.

The thrust cutting forces and torques of the tapping operation of the CW724R is illustrated in Fig. 4. Focusing on Fig. 5 b, when the form tap was inserted into the hole, a transition regime was seen for 0.2 to 0.4 seconds. The procedure was halted and reversed in the second of 1.4, leading to the taps returning and a large decrease in the force values. Similar to full immersion of the tapping, the return likewise exhibits a proportional constant zone with a cylindrical component and a slope. The torque increases asymptotically in region I of the torque graph, which represents the point of contact between the surfaces of the tap and the workpiece. Region I's tapered design of the tap produces the thread profiles by causing material deformation. Contrarily, area II experiences a steadying of the torque. The maximum torque is measured at the end of region II, where it shows a slight variance that may have resulted from friction variation. It should be highlighted that area III experiences an abrupt decrease in effort as a result of the process of tapping coming to an end. Region IV has a reversed tap spindle speed and entirely withdrawn tap returns from the hole. Additionally, in area IV, it should be noticed that the spindle's reversal counteracted the force applied in the forward direction before the tap emerged from the hole. On the other hand, when the operation was carried out deploying cut tap, the graph is formed of two regions: the engagement of the conical profile and then the hole diameter. The F+Ann. CW511L was machined utilizing cut and form taps, and the greatest thrust forces were measured as 183.7 N and 872.6 N, respectively. The lowest values, however, for Ext. CW617N were recorded at 110.3 and 660.5 N, respectively, utilizing cut and form taps. The same pattern was seen for the torque values of 711.98 N.m. and 29.83 N.m. in F+Ann. CW511L. Additionally, utilizing cut and form taps, the lowest values were determined to be 6.13 N.m and 14.64 Ext. CW617N, respectively. It is clear that the plastic movement of the material without chip removal in form taps led to larger frictional forces and coefficients, which in turn resulted in thrust forces and torque values that are almost four times those of cut taps. The F+Ann. specimens had greater measured thrust cutting forces and torques than the Ext. specimens. This phenomenon is primarily caused by an increase in the β-phase in the microstructure of CW617N and CW511L acquired by applied forging and annealing processes as well as κ-phase in the CW724R. It is obvious that the presence of Pb results in lower cutting forces and torques by retaining more lubricant on its surface, assisting in the decrease of wear or friction during contact. The measured thrust force and torque values were lower in CW724R than CW511L, despite the decreased Pb content. This is explained by the melting points of CW724R and CW511L, which are 600 and 900°C, respectively. Because of all this, softening during machining may also account for the reduced cutting forces of CW724R compared to CW511L. The silicon-rich κ -phase in the material's microstructure is another factor that contributes to the achieved result. In silicon-free brasses, the κ -phase is harder than the α- and β-phase and also has a BCC lattice structure, supporting the findings of [7].

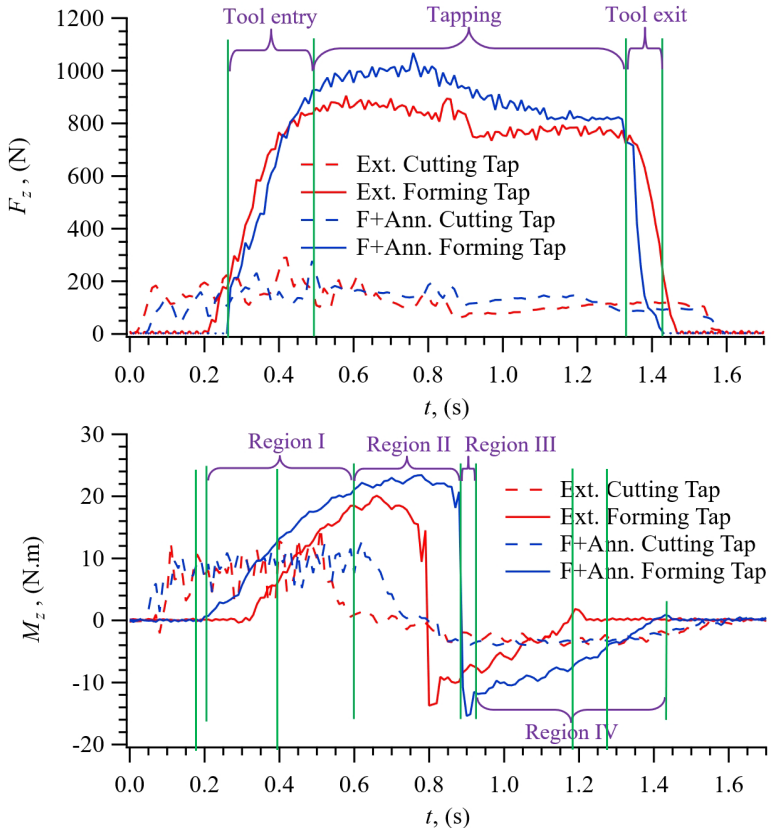

Fig. 4. The measured cutting forces and torques for CW724R.

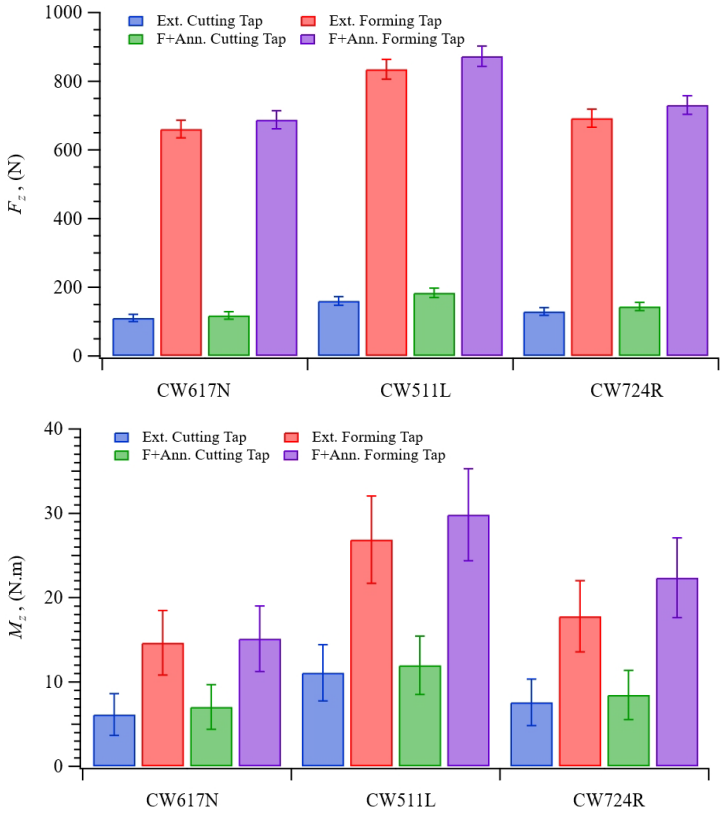

Fig. 5. The measured cutting forces and toques during the experiments.

Surface Quality Analysis and Geometrical Characteristics.

In the form tapping operation, on the top of the threads a split crest was observed due to no metallographic transformation. As demonstrated in Fig. 6b, the highest zone of deformation takes place in Z2 thread's root which during formation is in direct contact with the lobes. The work material flows from Z2 to Z3 on the flank of the thread which is a highly deformed zone and experiences significant displacements. In Z4 no significant deformation is observed. In the cutting tapping operation as shown in Fig. 6a, the thread form was achieved by material removal. Therefore, there were no formed crests on the top of the threads, and the triangle shape was clearly seen. The thread pitch, thread angles, flank straightness and minor, major diameters were inspected by optical Mitutoyo Contracer as well as tap gauges. The geometrical characteristics of all the threads in terms of dimensional tolerances were confirmed by the carried-out inspections and it was determined that the only different zone is Z4 of the threads generated between the tools. The length of Z4 was higher in formed threads than cut ones. It was seen that although in the dimensional tolerance range, the Z4 area in F+Ann. forming threads were much smoother as compared to Ext. specimens which might be attributed to the change in the materials' microstructure in terms of deformation, dislocation, phase content and microhardness. However, no remarkable differences in shape of the threads generated with the cutting tap were observed in all the experiments. Furthermore, some impurities and chip marks were observed on the surfaces Ext. CW511L and CW724R. On the other hand, the quality of the thread surfaces of the CW617N was excellent. The highest impurities belong to CW511L which is also as verification to the force measurements of this paper.

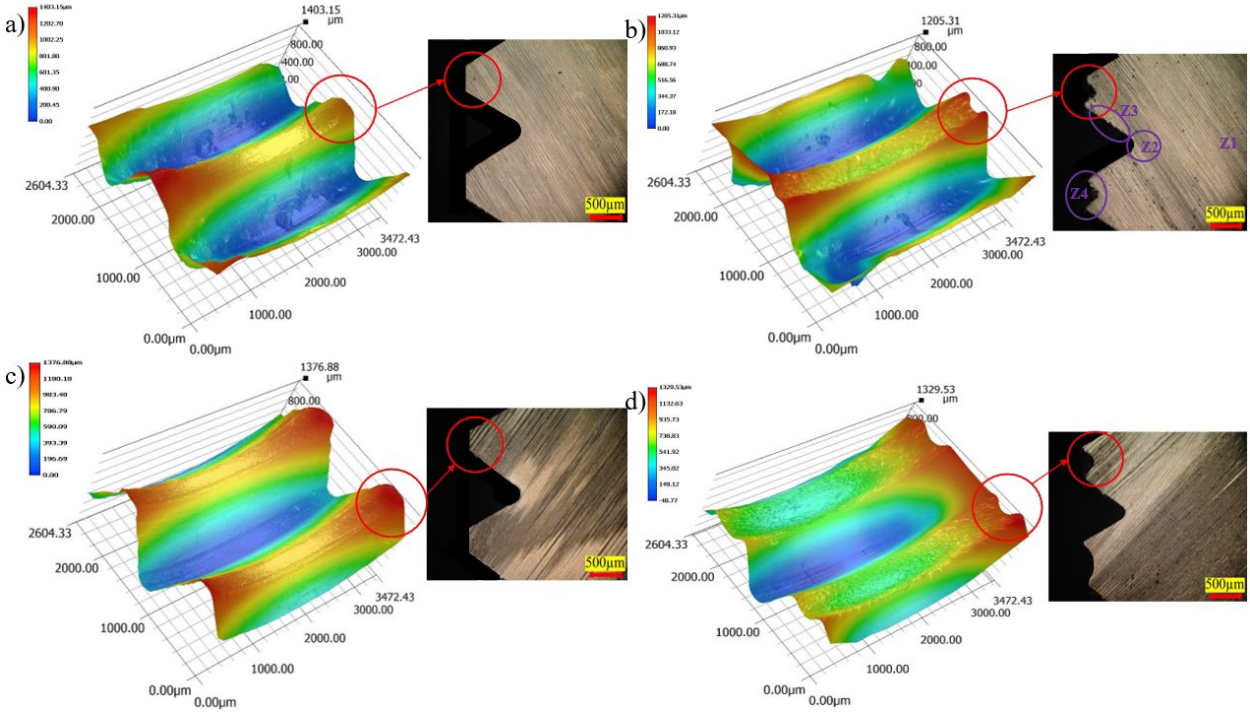

Fig. 6. The formed threads; Ext. CW511L a) cutting, b) forming, F+Ann. CW511L c) cutting, d) forming.

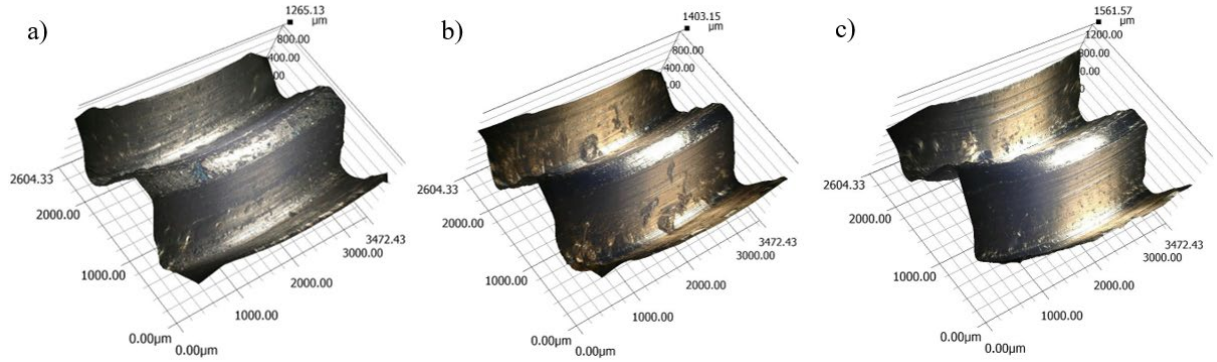

Fig. 7. The cut threads on Ext.; a) CW617N, b) CW511L, c) CW724R.

Surface and Subsurface Microhardness Analysis.

Fig. 8 shows the measured machined surface and sub-surface microhardness of the threads in at 0, 15, 30, 50, 75, 150, 300 and 600 µm distances from the surface. All measurements have been carried out from the most deformed zone, the root of the thread and the average value of two measurements is reported. The properties of the base material could be assessed 600 µm beneath the surface due to the generated strain hardening. The highest microhardness was measured at the machined surface of F+Ann. CW511L with %234.6 increase with respect to the base material using cutting tap. Tapping with cutting tool resulted in higher variations in the surface and sub-surface microhardness. The obtained results show that the tapping tool type plays a significant role in the sub-surface strain hardening. This phenomenon is generated by the deformation of the material structure by the friction and forces between tap and work specimen.

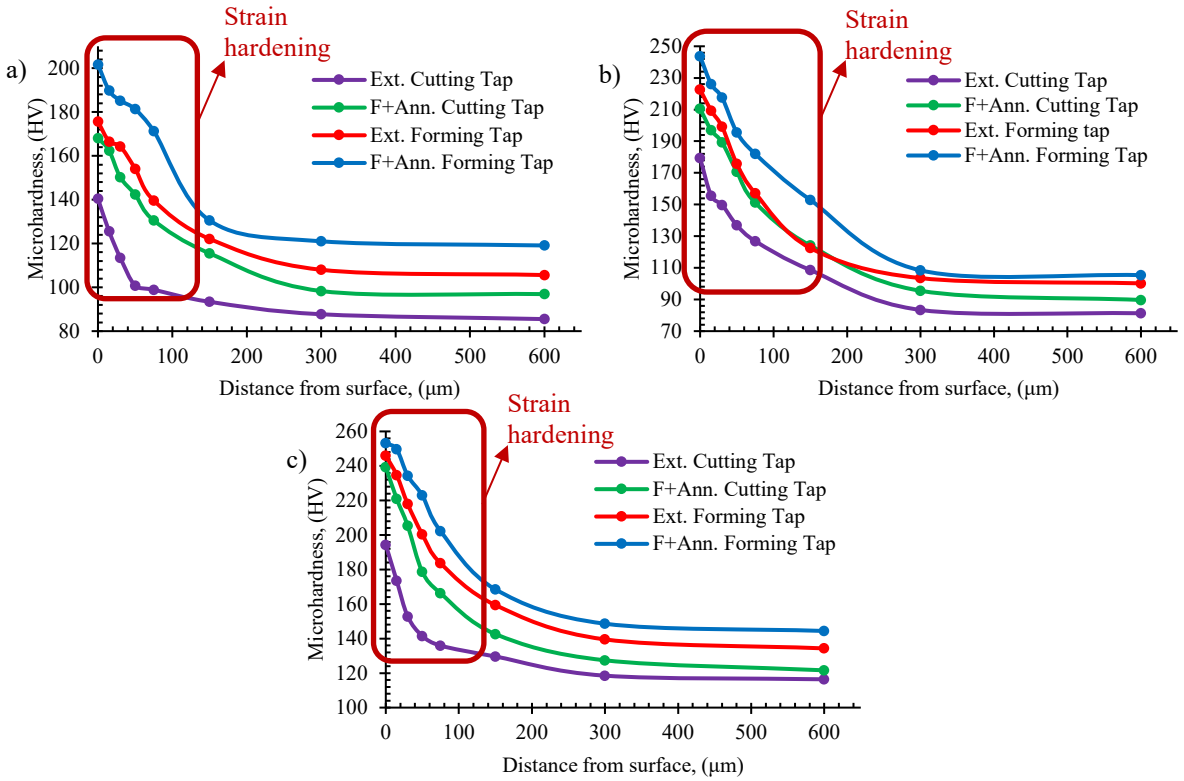

Fig. 8. The measured machined surface and sub-surface microhardness; a) CW617N, b) CW511L, c) CW724R.

Summary
An investigation was carried out to compare cutting and forming tap tool efficiency with respect to thread accuracy, surface quality, generated cutting forces, torques and microhardness in internal threading operation on different types of lead-free brass alloys. Tool type, as well as materials manufacturing method were found to have a significant effect on surface integrity and process responses. In form tapping compared to cutting, higher cutting forces and torques were recorded. It was observed that the phase contents and grain refinement were obtained by multi-directional hot forging operation in the test specimens' microstructure.
The cutting tap tool determined higher strain hardening, but lower thickness of the plastically deformed sub-surface layer and enhanced thread quality in terms of form and dimension.

Acknowledgements
The authors thank TUBITAK (The Scientific and Technological Research Council of Turkey) for partially supporting this work under project number 118C069.

References
[1] N. Zoghipour, E. Tascioglu, G. Atay, Y. Kaynak, Machining-induced surface integrity of holes drilled in lead-free brass alloy, Procedia CIRP 87 (2020) 148-152. https://doi.org/10.1016/j.procir.2020.02.102
[2] Information on:
https://rohs.exemptions.oeko.info/fileadmin/user_upload/RoHS_Pack_9/Exemption_6_c_/
[3] G.M. Sicoe, D. Iacomi, M. Iordache, E. Nitu, Research on numerical modelling and simulation of the form tapping process to achieve profiles, Int. J. Modern Manuf. Technol. 5 (2013).
[4] G. Fromentin, G. Poulachon, A. Moisan, Thread forming tapping of alloyed steel, ICME Proceedings, Naples, Italy, 2002, pp. 115-118.
[5] G. Fromentin, G. Poulachon, A. Moisan, B. Julien, J. Giessler, Precision and surface integrity of threads obtained by form tapping, CIRP Annals 54 (2005) 519-522. https://doi.org/10.1016/S0007-8506(07)60159-0
[6] V. Ivanov, V. Kirov, Rolling of internal threads: part 1, J. Mater. Process. Technol. 72 (1996) 214–220.
[7] J.S. Agapiou, Evaluation of the effect of high-speed machining on tapping, J. Manuf. Sci. Eng. Technol. ASME 116 (1994) 457- 462.
[8] V. Ivanov, Rolling of internal threads: Part 2, J. Mater. Process. Technol. 72 (1996) 221-225.
[9] S. Chowdhary, S.G. Kapoor, R.E. DeVor, Modeling forces including elastic recovery for internal thread forming, J. Manuf. Sci. Eng. ASME 125 (2003) 681-688. https://doi.org/10.1115/1.1619178
[10] R. Chandra, S.C. Das, Forming taps and their influence on production, J. India Eng. 1975.
[11] G. Fromentin, G. Poulachon, A. Moisan, Metallurgical aspects in cold forming tapping, NCMR Proceedings, Leeds, UK, 2002, pp. 373-377.
[12] G. Uzun, I. Korkut, The effects of cutting conditions on the cutting torque and tool life in the tapping process for AISI 304 stainless steel, Mater. Technol. 50 (2016) 275–280. http://doi.org/10.17222/mit.2015.044
[13] J.A. de Oliveira, S.L.M. R. Filho, L.C. Brandão, Investigation of the influence of coating and the tapered entry in the internal forming tapping process, Int. J. Adv. Manuf. Technol. 101 (2018) 1051-1063.
[14] S.L.M. R. Filho, J.A. de Oliveira, É.M. Arruda, L.C. Brandão, Analysis of burr formation in form tapping in 7075 aluminum alloy, Int. J. Adv. Manuf. Technol. 84 (2015). http://doi.org/10.1007/s00170-015-7768-9

[15] W. Belluco, L. De Chiffre, Surface integrity and part accuracy in reaming and tapping stainless steel with new vegetable based cutting oils, Tribol. Int. 35 (2002) 865-870. http://doi.org/10.1016/S0301-679X(02)00093-2
[16] C.C.F. Coelho, R.B.D. Pereira, C.H. Lauro, L.C. Brandao, Performance evaluation of tapping processes using a 7075 aluminium alloy with different cooling systems and threading heads, Proc IMechE Part C: J. Mech. Eng. Sci. 203-210 (2019). http://doi.org/10.1177/0954406219867730
[17] H.J. Patel, B,P, Patel, S,M, Patel, A review on thread tapping operation and para-metric studym Int, J, Eng, Res, Appl. 2 (2012) 109–113.
[18] EMUGE-FRANKEN, Threading Technology, InnoForm Cold-forming Taps - Chipless production of internal threads, Germany, 2009, 28.
[19] ISO 68-1:1998 – a (1998a) ISO general purpose screw threads—basic profile—Part 1: metric screw threads, 1ft ed, pp. 3.
[20] ISO 68-2:1998 – b (1998b) ISO general purpose screw threads—basic profile—Part 2: metric screw threads, 1ft ed., pp. 4.
[21] Information on http:\\www.sarbak.com\document\pdf